

Electronic Supplementary Information

Synthesis, Structural Characterization, Solvatochromism, and Ion-binding Studies of a Ditopic Receptor Based on 2-(4-[2,2':6',2'']Terpyridin-4'-yl-phenyl)-1*H*-phenanthro[9,10-*d*] imidazole (tpy-HImzphen) Unit

Chanchal Bhaumik, Dinesh Maity, Shyamal Das, and Sujoy Baitalik*

Department of Chemistry, Inorganic Chemistry Section, Jadavpur University, Kolkata – 700032, India

E-mail: sbaitalik@hotmail.com

Table S1 All bond distances (Å) for tpy-HImzphen

tpy-HImzphen							
O(1)-C(38)	1.216(4)	C(35)-C(36)	1.395(4)	C(26)-C(25)	1.403(4)	C(12)-C(13)	1.364(5)
N(1)-C(22)	1.325(4)	C(34)-C(35)	1.370(4)	C(25)-C(24)	1.438(4)	C(11)-C(12)	1.376(4)
N(1)-C(24)	1.382(3)	C(33)-C(34)	1.385(5)	C(24)-C(23)	1.368(4)	C(10)-C(11)	1.479(4)
N(2)-C(22)	1.365(3)	C(33)-C(32)	1.363(4)	C(22)-C(19)	1.454(4)	C(8)-C(9)	1.388(4)
N(2)-C(23)	1.370(4)	C(36)-C(31)	1.421(4)	C(20)-C(21)	1.382(4)	C(8)-C(7)	1.390(4)
N(3)-C(15)	1.334(5)	C(36)-C(23)	1.430(4)	C(16)-C(21)	1.391(4)	C(7)-C(6)	1.392(4)
N(3)-C(11)	1.339(4)	C(31)-C(32)	1.405(4)	C(19)-C(20)	1.384(4)	C(6)-C(5)	1.489(4)
N(4)-C(10)	1.348(4)	C(30)-C(31)	1.465(4)	C(19)-C(18)	1.380(4)	C(5)-C(4)	1.382(4)
N(4)-C(6)	1.330(4)	C(29)-C(30)	1.408(4)	C(18)-C(17)	1.386(4)	C(3)-C(4)	1.383(5)
N(5)-C(5)	1.340(4)	C(28)-C(29)	1.362(5)	C(17)-C(16)	1.374(4)	C(2)-C(3)	1.359(5)
N(5)-C(1)	1.337(4)	C(28)-C(27)	1.385(4)	C(16)-C(8)	1.480(4)	C(1)-C(2)	1.358(5)
C(38)-C(39)	1.505(5)	C(27)-C(26)	1.366(4)	C(14)-C(15)	1.358(6)		
C(37)-C(38)	1.484(5)	C(25)-C(30)	1.419(4)	C(13)-C(14)	1.370(6)		

Table S2 All bond angles (deg) for tpy-HImzphen

tpy-HImzphen					
C(22)-N(1)- C(24)	104.2(2)	C(17)-C(16)- C(8)	122.8(3)	C(31)-C(36)- C(23)	116.3(3)
C(22)-N(2)- C(23)	107.0(2)	C(21)-C(16)- C(8)	120.3(3)	C(24)-C(23)- C(36)	124.2(3)
C(1)-N(5)- C(5)	116.9(3)	C(9)-C(8)- C(7)	116.7(3)	N(2)-C(23)- C(36)	130.3(3)
C(15)-N(3)- C(11)	116.9(3)	C(9)-C(8)- C(16)	122.4(3)	C(28)-C(29)- C(30)	121.3(3)
C(29)-C(28)- C(27)	121.3(3)	C(7)-C(8)- C(16)	120.9(3)	C(29)-C(30)- C(25)	117.0(3)
C(26)-C(27)- C(28)	119.5(3)	C(8)-C(9)- C(10)	120.1(3)	C(31)-C(30)- C(29)	122.0(3)
C(27)-C(26)- C(25)	120.6(3)	N(4)-C(10)- C(9)	122.8(3)	C(32)-C(31)- C(36)	116.3(3)
C(26)-C(25)- C(30)	120.2(3)	N(4)-C(10)- C(11)	116.1(3)	C(32)-C(31)- C(30)	123.4(3)
C(26)-C(25)- C(24)	122.5(3)	C(9)-C(10)- C(11)	121.1(3)	C(36)-C(31)- C(30)	120.3(3)
C(30)-C(25)- C(24)	117.3(3)	N(3)-C(11)- C(12)	122.0(3)	C(33)-C(32)- C(31)	122.5(3)
N(1)-C(24)- C(23)	111.1(2)	N(3)-C(11)- C(10)	117.1(3)	C(21)-C(20)- C(19)	121.6(3)
N(1)-C(24)- C(25)	128.0(3)	C(12)-C(11)- C(10)	121.0(3)	C(20)-C(21)- C(16)	121.1(3)
C(23)-C(24)- C(25)	120.9(3)	C(20)-C(21)- C(16)	121.2(2)	C(8)-C(7)- C(6)	119.9(3)
N(1)-C(22)- N(2)	112.2(2)	C(13)-C(12)- C(11)	119.6(4)	N(4)-C(6)- C(7)	123.2(3)
N(1)-C(22)- C(19)	124.3(2)	C(12)-C(13)- C(14)	119.0(4)	N(4)-C(6)- C(5)	116.6(3)
N(2)-C(22)- C(19)	123.5(2)	C(15)-C(14)- C(13)	118.0(4)	C(7)-C(6)- C(5)	120.2(3)
C(18)-C(19)- C(20)	117.2(3)	C(32)-C(33)- C(34)	120.1(3)	N(5)-C(5)- C(4)	121.7(3)
C(18)-C(19)- C(22)	123.2(3)	C(35)-C(34)- C(33)	119.8(3)	N(5)-C(5)- C(6)	116.8(3)
C(20)-C(19)- C(22)	119.6(2)	C(34)-C(35)- C(36)	120.7(3)	C(4)-C(5)- C(6)	121.5(3)
C(19)-C(18)- C(17)	121.1(3)	C(35)-C(36)- C(31)	120.4(3)	N(5)-C(1)- C(2)	124.8(4)
C(16)-C(17)- C(18)	122.0(3)	C(35)-C(36)- C(23)	123.3(3)	C(32)-C(33)- C(34)	119.1(3)
C(17)-C(16)- C(21)	116.9(3)	C(24)-C(23)- N(2)	105.5(2)	C(1)-C(2)- C(3)	118.3(4)
C(2)-C(3)- C(4)	118.8(3)	C(5)-C(4)- C(3)	119.6(3)	C(6)-N(4)- C(10)	117.2(2)
N(3)-C(15)- C(14)	124.5(4)	C(37)-C(38)- C(39)	115.7(3)		
O(1)-C(38)- C(39)	122.9(3)	O(1)-C(38)- C(37)	121.5(3)		

Table S3. Epsilon (ϵ) values of complexes for different M^{2+} metal ions at three different wavelengths.

$[M(\text{tpy}-\text{HImzPh}_3)_2]^{2+}$	ϵ Values in $M^{-1}\text{cm}^{-1}$		
	At 575 nm	At 520 nm	At 320 nm
Mn	0	0	54910
Fe	45050	14340	70270
Co	1010	5400	65630
Ni	0	8	55540
Cu	230	610	58480
Zn	0	40	45360
Cd	0	0	56360
Pb	0	0	58220

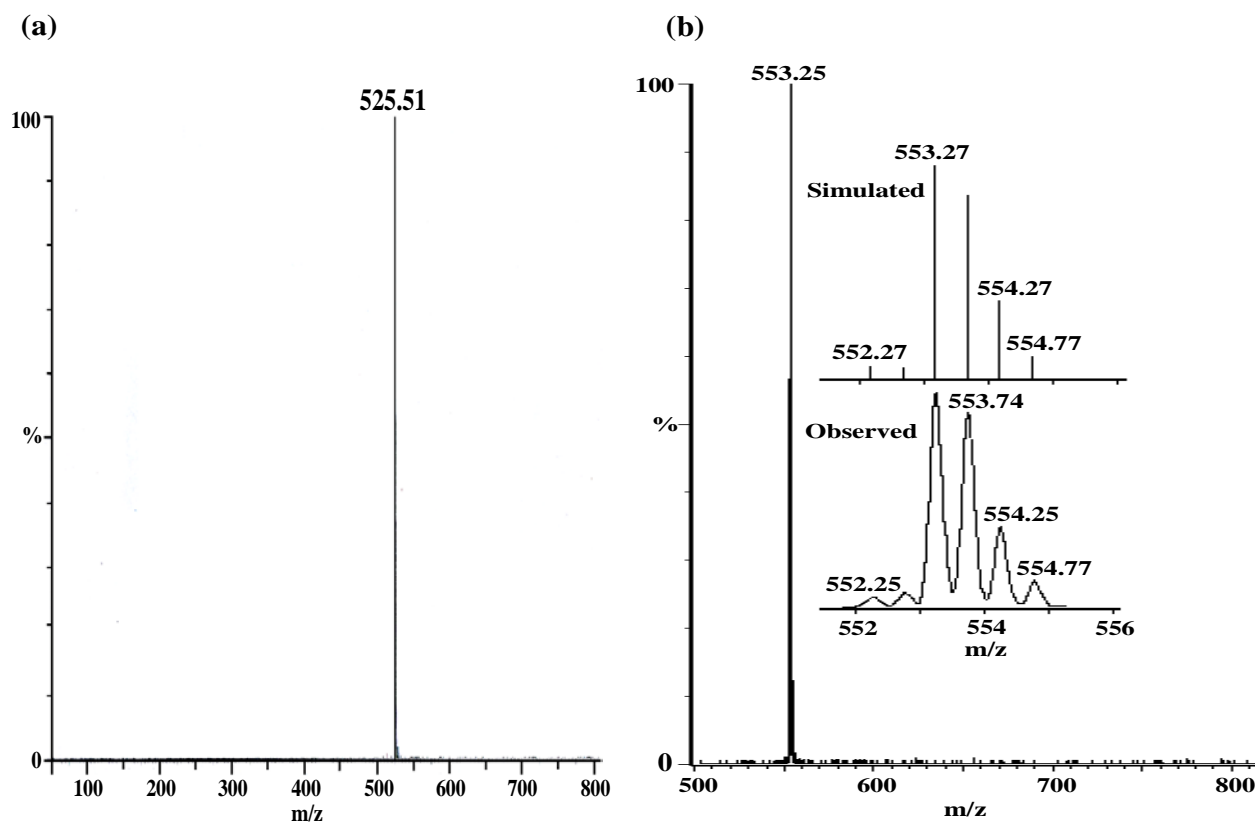


Fig. S1 ESI-MS for (a) tpy-HImzphen ($m/z = 525.51$) in dimethylformamide and (b) complex cation $[\text{Fe}(\text{tpy-HImzphen})_2]^{2+}$ ($m/z = 553.25$) in acetonitrile showing the observed and simulated isotopic distribution patterns.

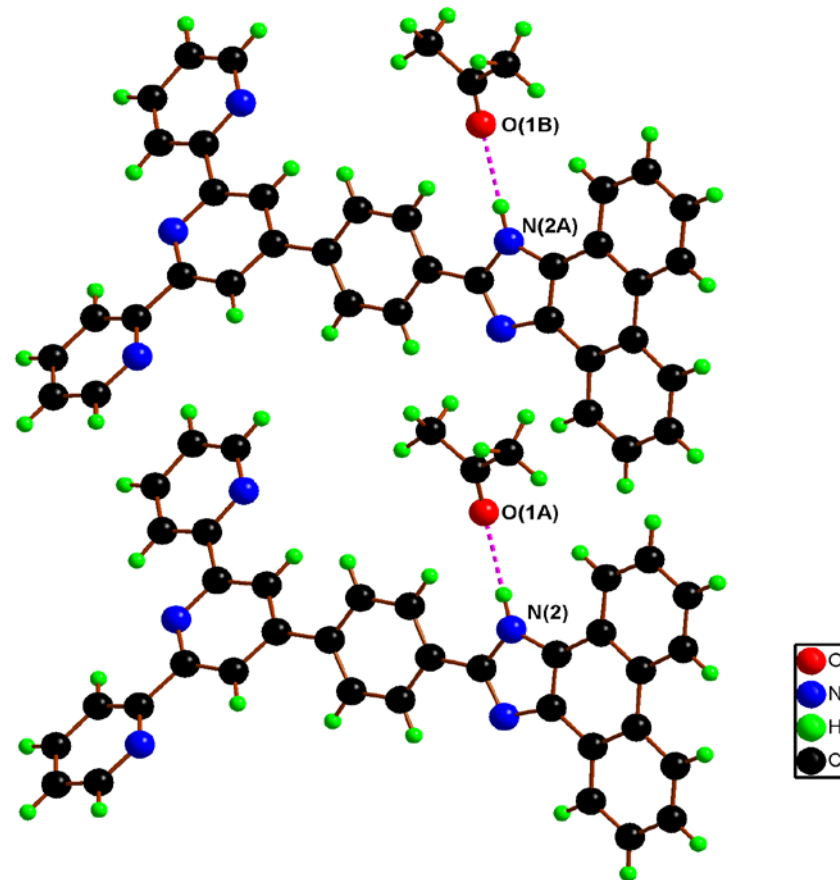


Fig. S2 Intermolecular hydrogen-bonding interaction between the imidazole N-H proton of the receptor and the solvent acetone molecule.

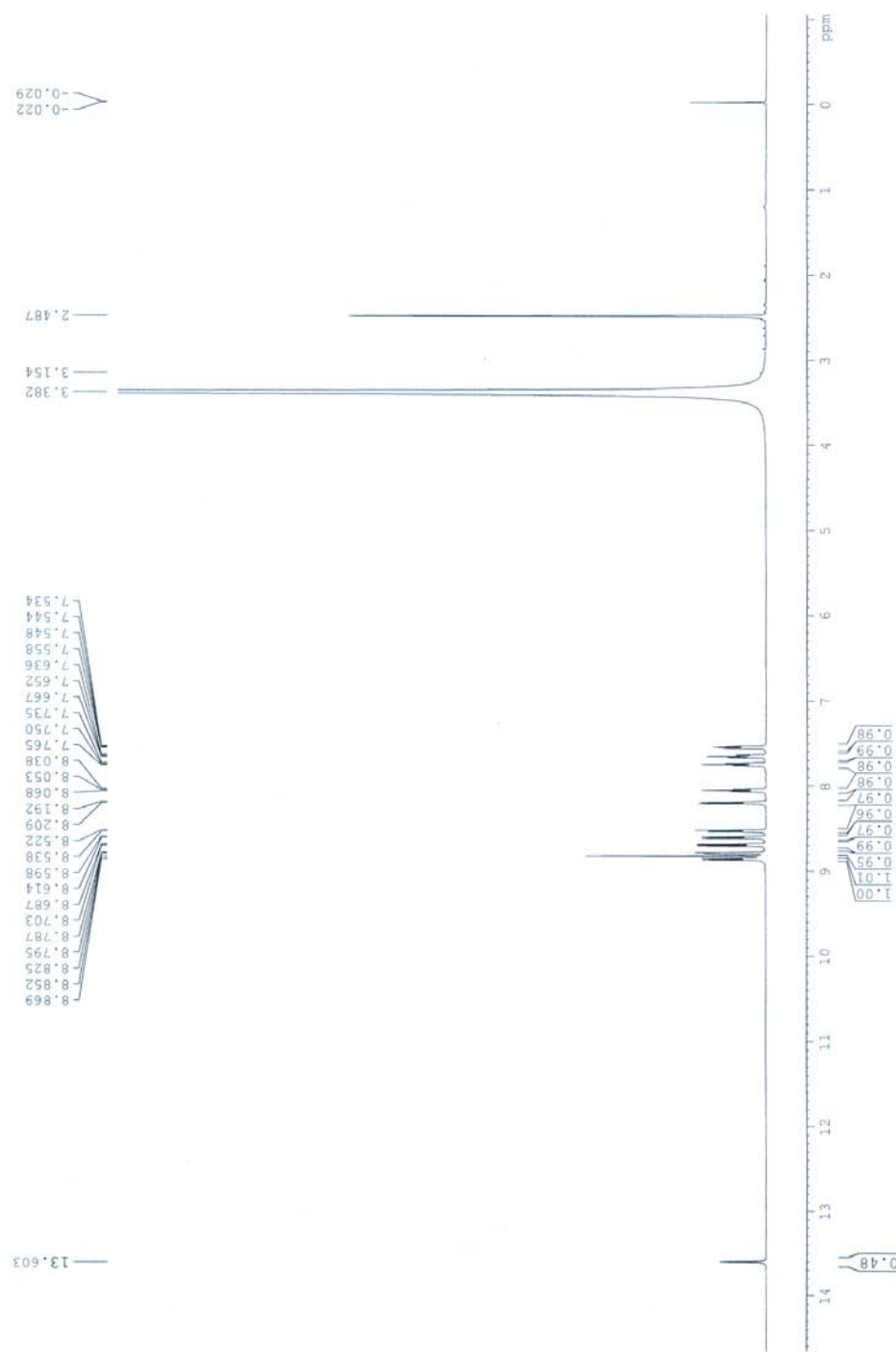


Fig. S3 ¹H NMR spectra of the receptor in DMSO-*d*₆.

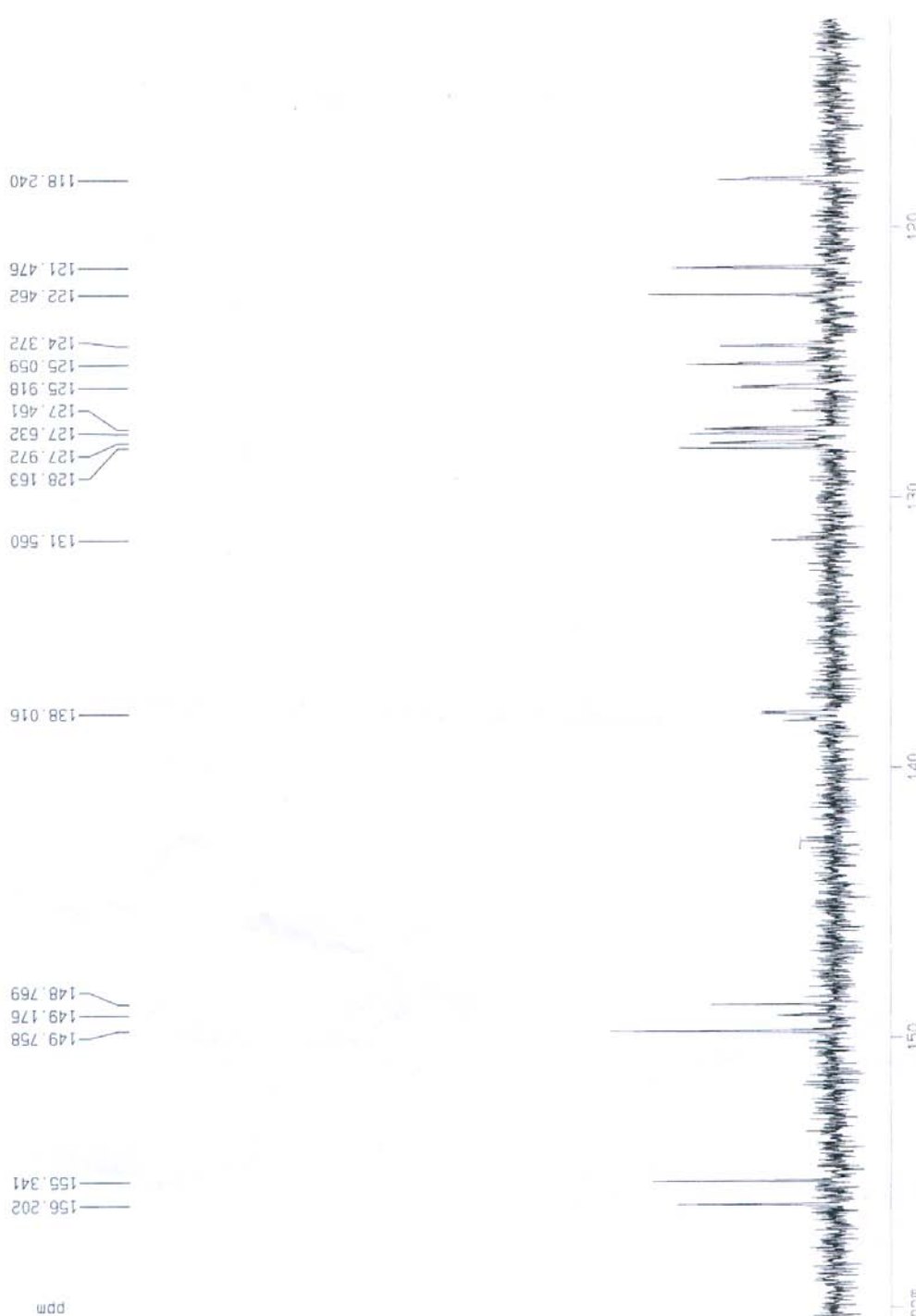


Fig. S4 ^{13}C NMR spectra of the receptor in $\text{DMSO}-d_6$.

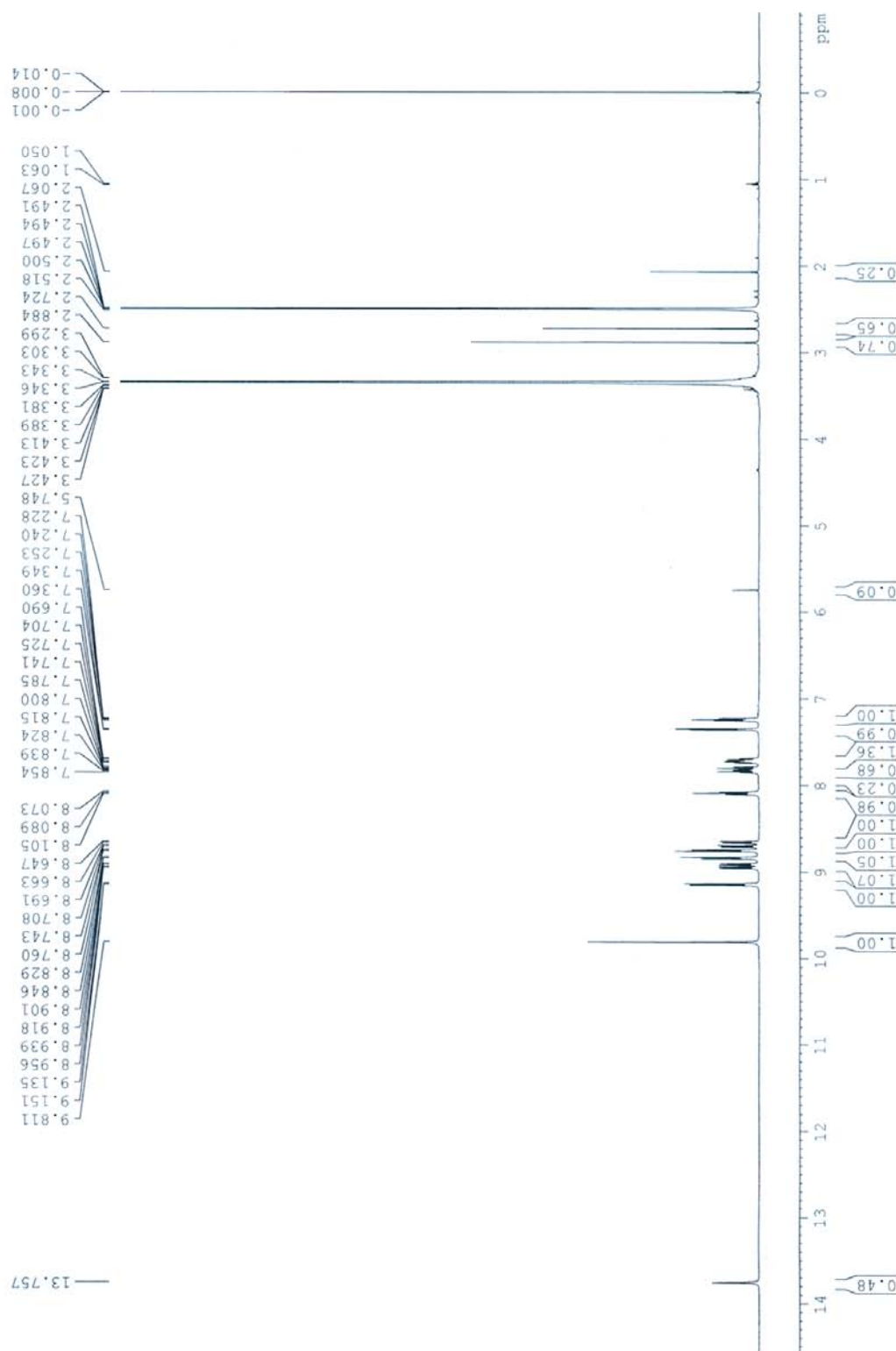


Fig. S5 ^1H NMR spectra of $[\text{Fe}(\text{tpy}-\text{HImzphen})_2](\text{ClO}_4)_2$ in $\text{DMSO}-d_6$.

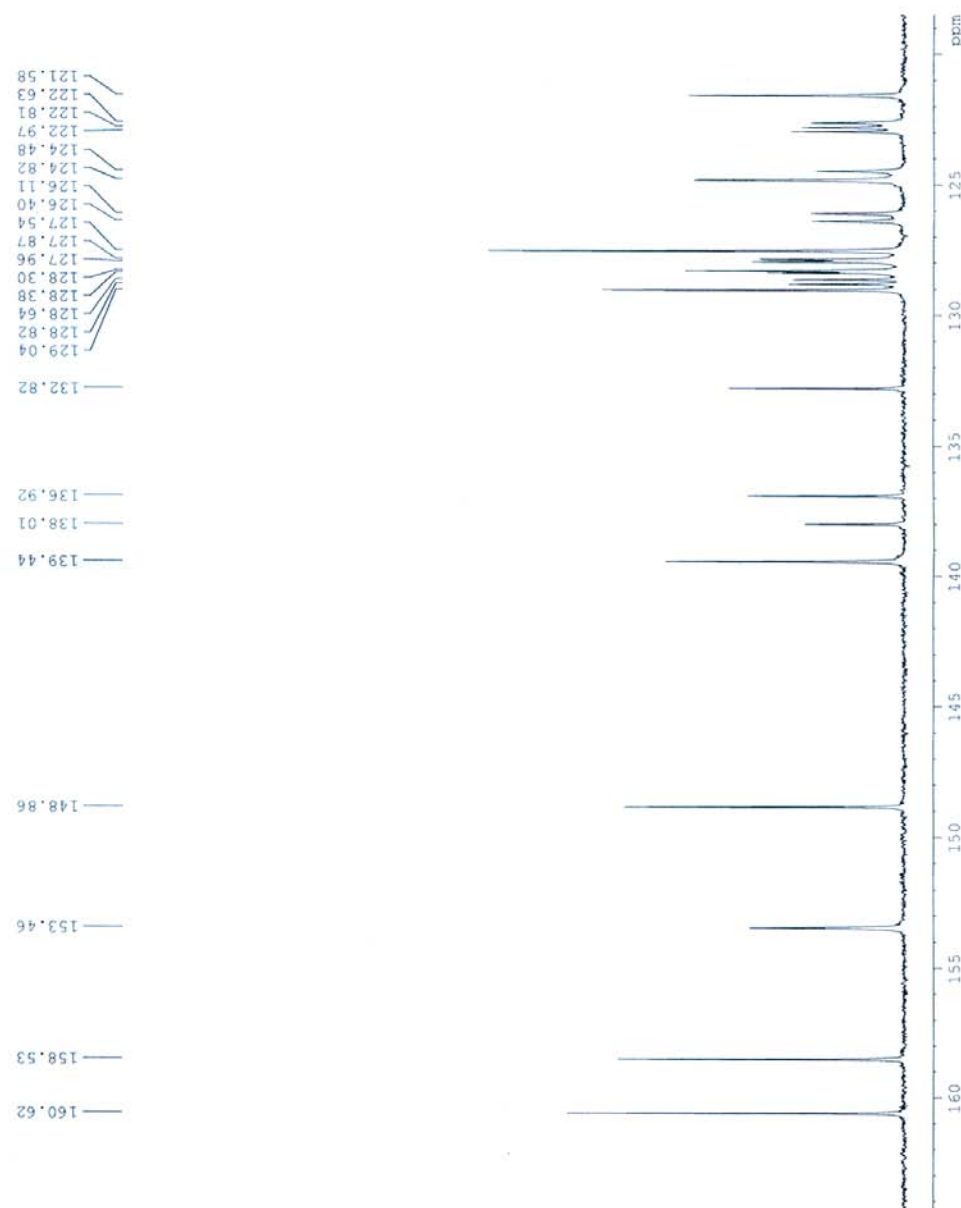


Fig. S6 ^{13}C NMR spectra of $[\text{Fe}(\text{tpy-HImzphen})_2](\text{ClO}_4)_2$ in $\text{DMSO}-d_6$.

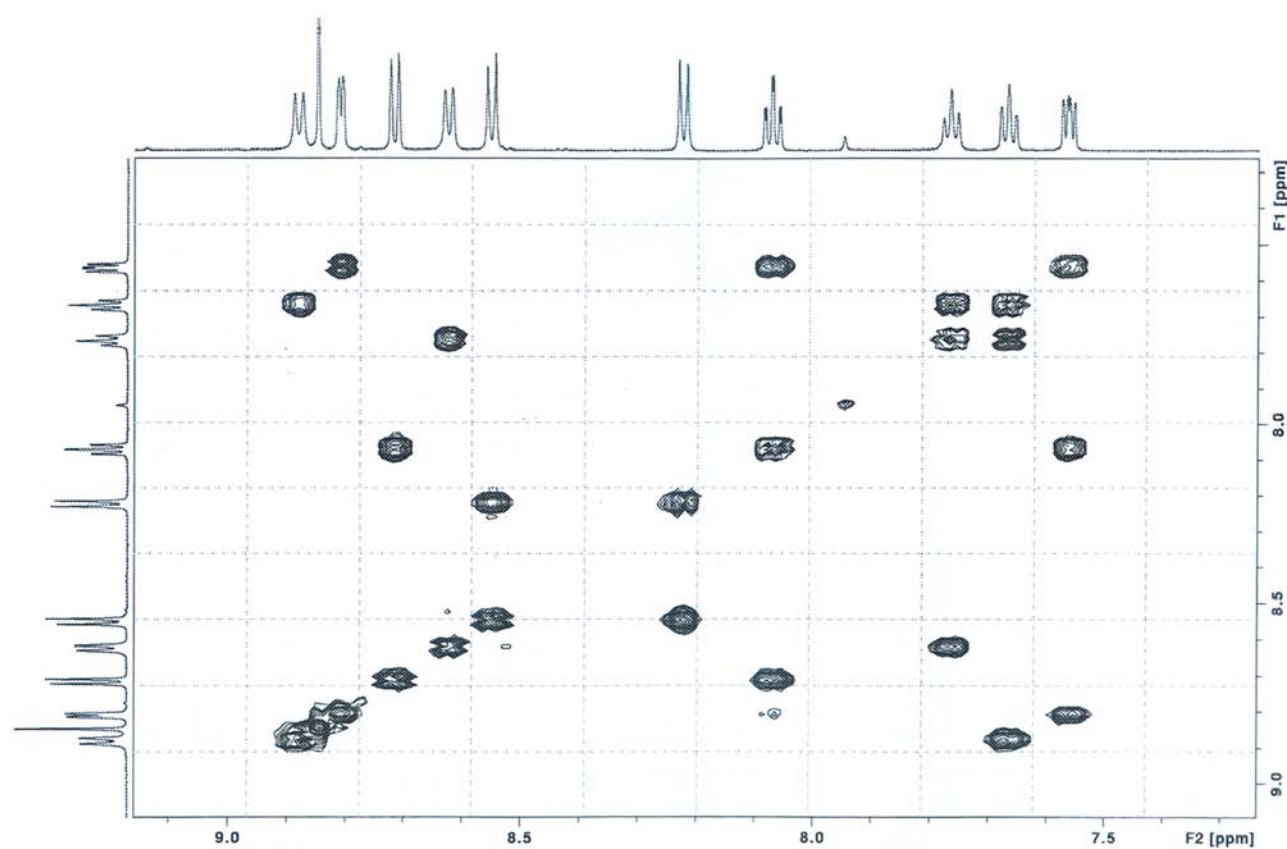


Fig. S7 $\{^1\text{H}-^1\text{H}\}$ COSY NMR spectrum of the receptor in $\text{DMSO}-d_6$.

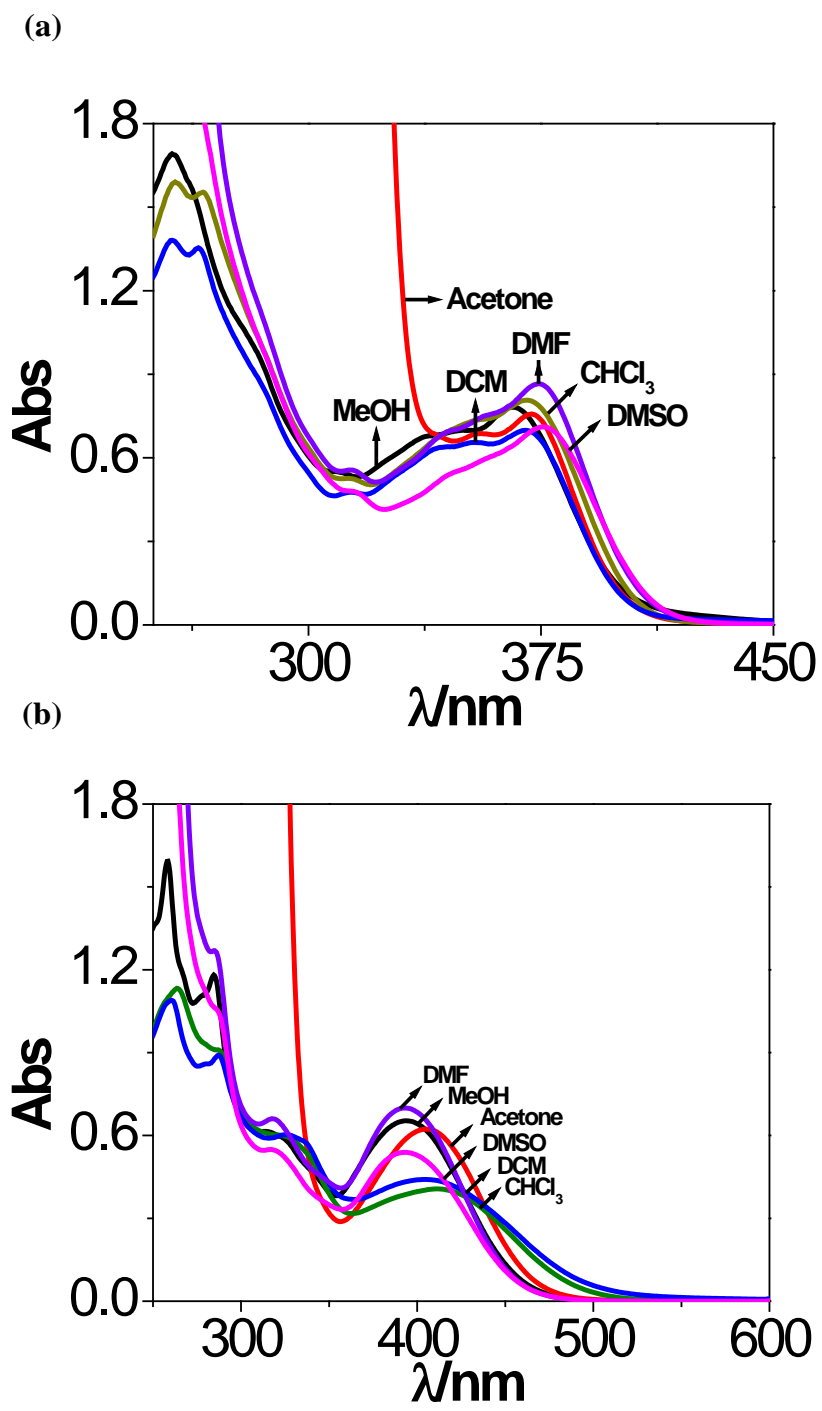


Fig. S8 UV-vis spectra of the receptor tpy-HImzphen (a) and its Zn(II) complex $[\text{Zn}(\text{tpy}-\text{HImzphen})_2]^{2+}$ (b) in different solvents.

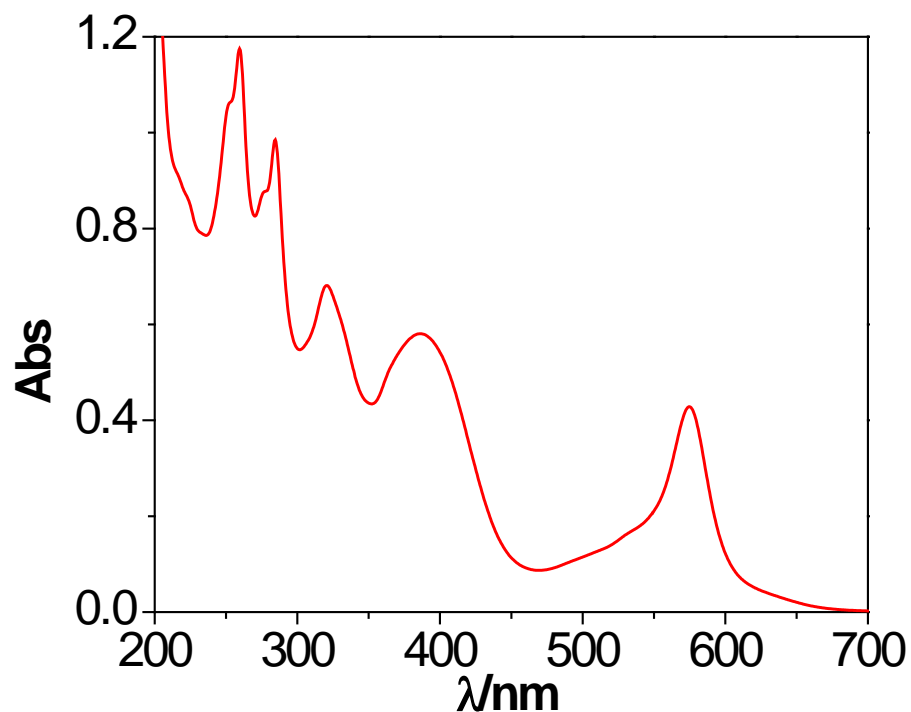


Fig. S9 UV-vis spectra of $[\text{Fe}(\text{tpy-HImzphen})_2]^{2+}$ in acetonitrile.

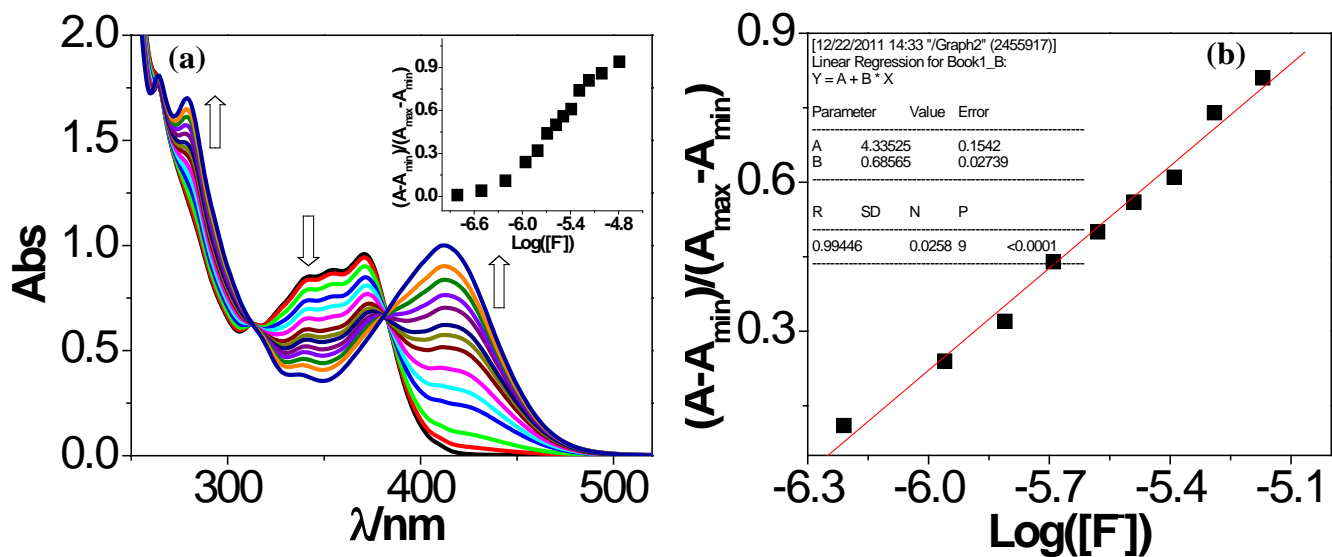


Fig. S10 (a) Absorbance changes during the titration of tpy-HImzphen (20 μM) with F^- (0-180 μM) in dimethylformamide-acetonitrile (1:9), inset: Normalized absorbance between the minimum absorbance (free tpy-HImzphen) and the maximum absorbance (180 μM F^- added). (b) A plot of $(A - A_{\min}) / (A_{\max} - A_{\min})$ vs $\text{Log}([\text{F}])$, the calculated detection limit of receptor is $5.4 \times 10^{-7} \text{ M}$.

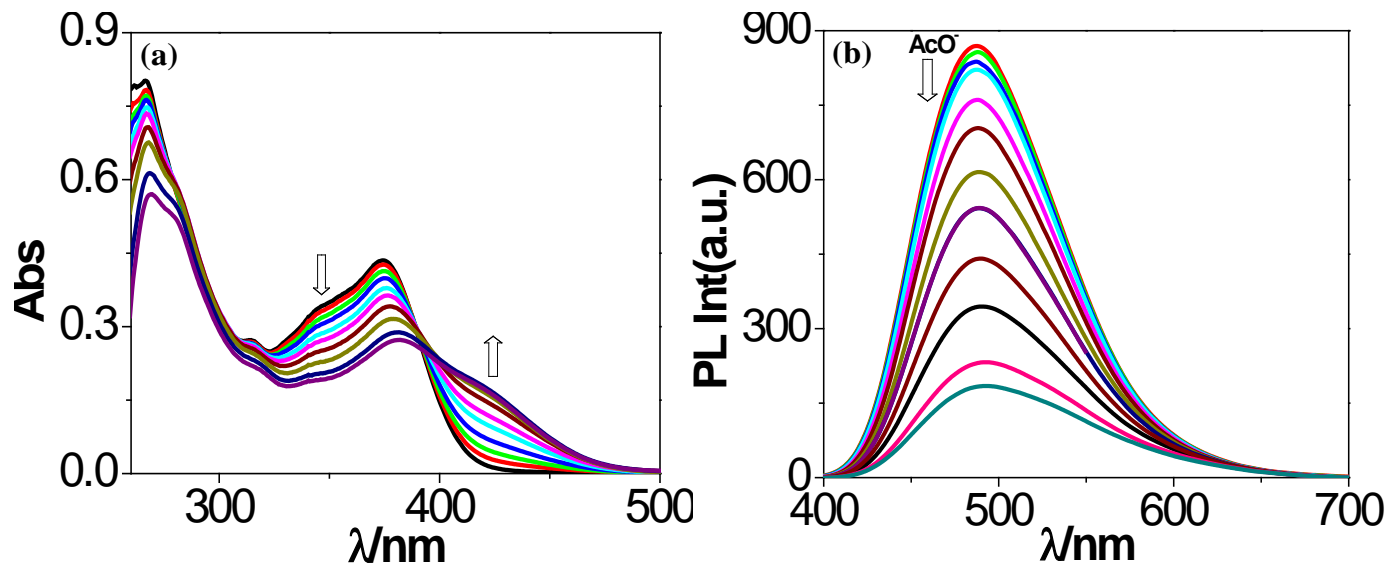


Fig. S11 Changes in UV-vis (a) and luminescence (b) spectra of tpy-HImzphen (20 μM) in dimethylformamide-acetonitrile (1:9) upon the addition of AcO^- ion (0-12000 μM).

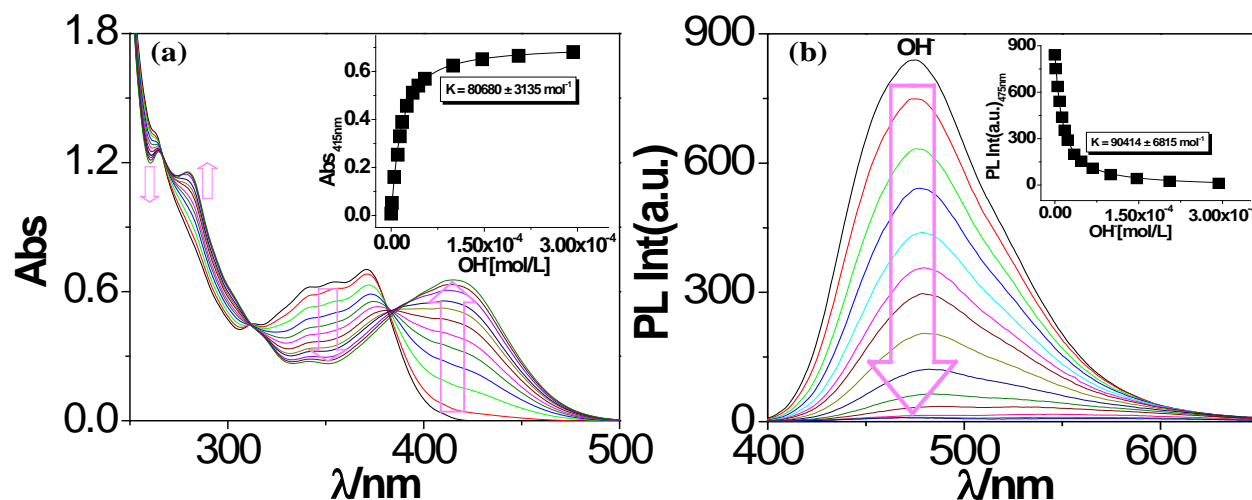


Fig. S12 Changes in UV–vis (a) and luminescence (b) spectra of tpy-HImzphen (20 μM) in dimethylformamide-acetonitrile (1:9) upon the addition of OH⁻ ion (0–200 μM). The inset shows the fit of the experimental absorbance and luminescence data to a 1:1 binding profile.

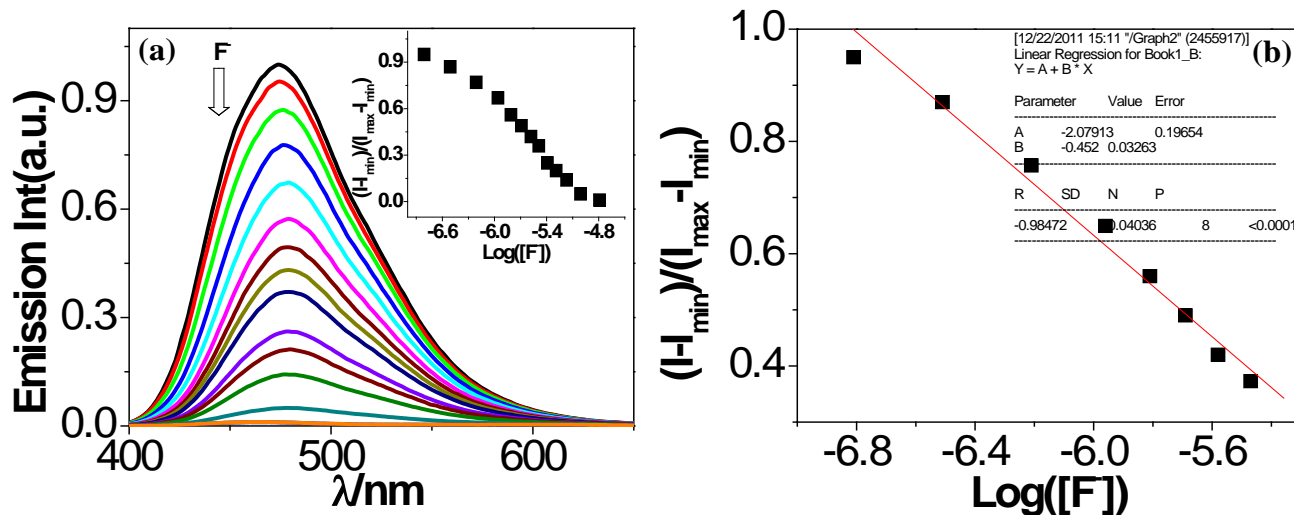


Fig. S13 (a) Fluorescence changes during the titration of tpy-HImzphen (20 μM) with F⁻ (0–180 μM) in dimethylformamide-acetonitrile (1:9), inset: Normalized intensity between the maximum intensity (free tpy-HImzphen) and the minimum intensity (180 μM F⁻ added). (b) A plot of (I - I_{min})/(I_{max} - I_{min}) vs Log([F⁻]), the calculated detection limit of receptor is 1.5×10^{-7} M.

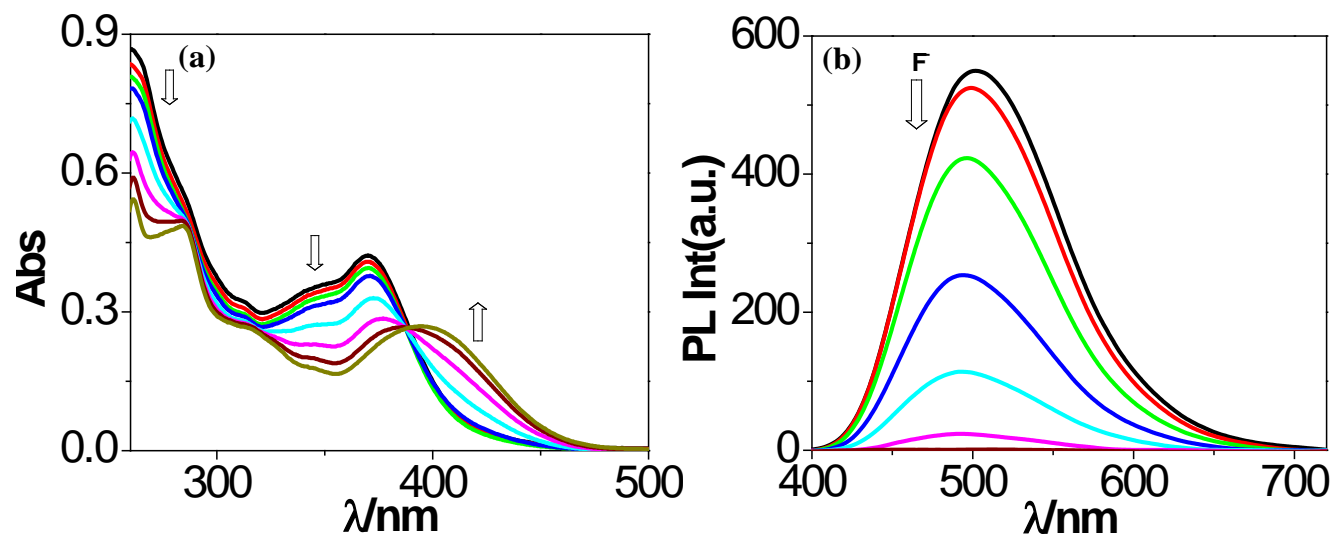


Fig. S14 Changes in UV-vis (a) and luminescence (b) spectra of tpy-HImzphen (20 μM) in dimethylsulfoxide-water (3:2) upon the addition of F⁻ ion (0–5000 μM). The inset shows the fit of the experimental absorbance and luminescence data to a 1:1 binding profile.

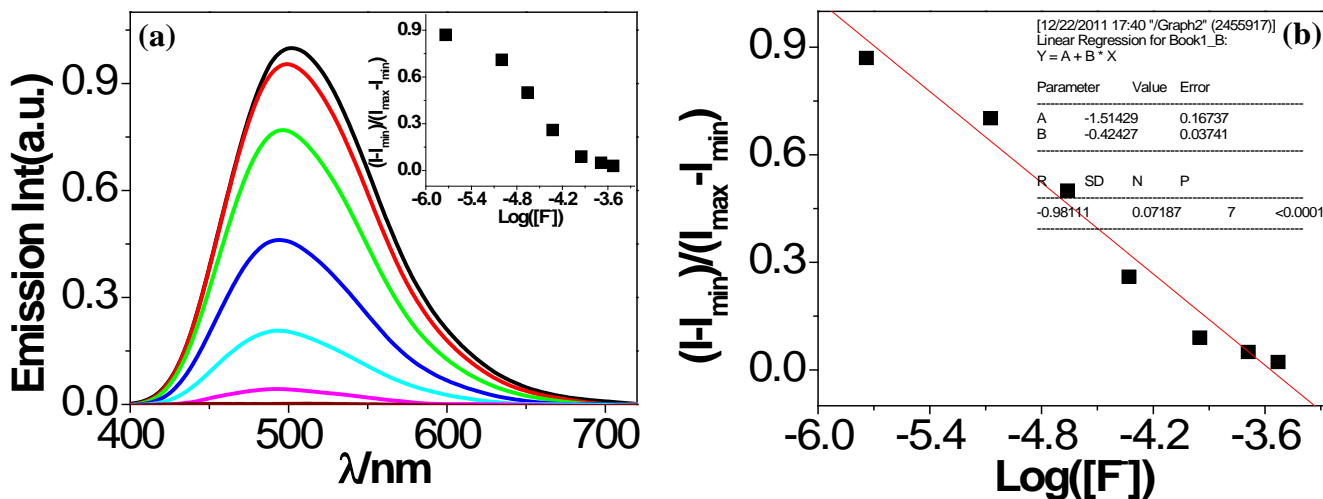


Fig. S15 a) Fluorescence changes during the titration of tpy-HImzphen (20 μM) with F⁻ (0–5000 μM) in dimethylsulfoxide-water (3:2), inset: Normalized intensity between the maximum intensity (free tpy-HImzphen) and the minimum intensity (5000 μM F⁻ added). b) A plot of $(I - I_{\min}) / (I_{\max} - I_{\min})$ vs Log([F⁻]), the calculated detection limit of receptor is 1.2×10^{-6} M.

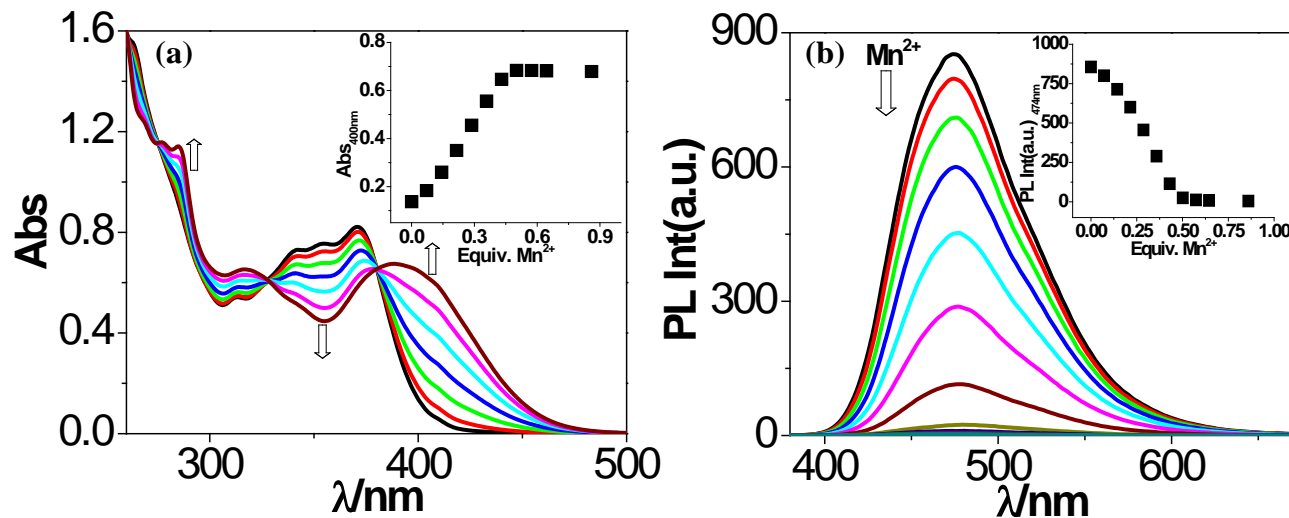


Fig. S16 Changes in UV-vis (a) and photoluminescence (b) spectra of tpy-HImzphen (20 μM) in dimethylformamide-acetonitrile (1:9) upon addition of Mn(ClO₄)₂ (20 μM). The inset shows the change of absorption and emission intensity as a function of the equivalent of Mn²⁺ ion added.

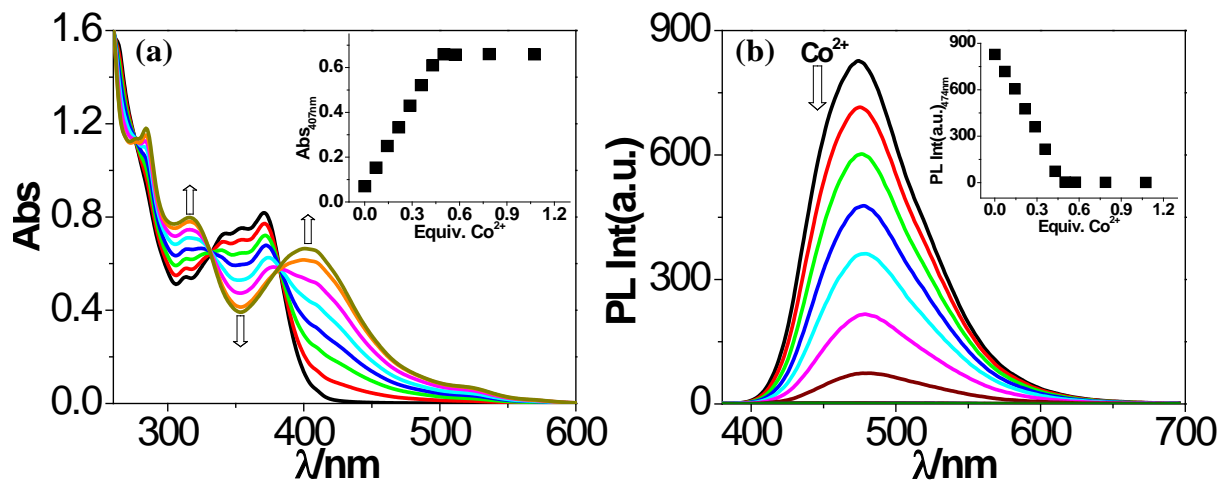


Fig. S17 Changes in UV-vis (a) and photoluminescence (b) spectra of tpy-HImzphen (20 μM) in dimethylformamide-acetonitrile (1:9) upon addition of Co(ClO₄)₂ (20 μM). The inset shows the change of absorption and emission intensity as a function of the equivalent of Co²⁺ ion added.

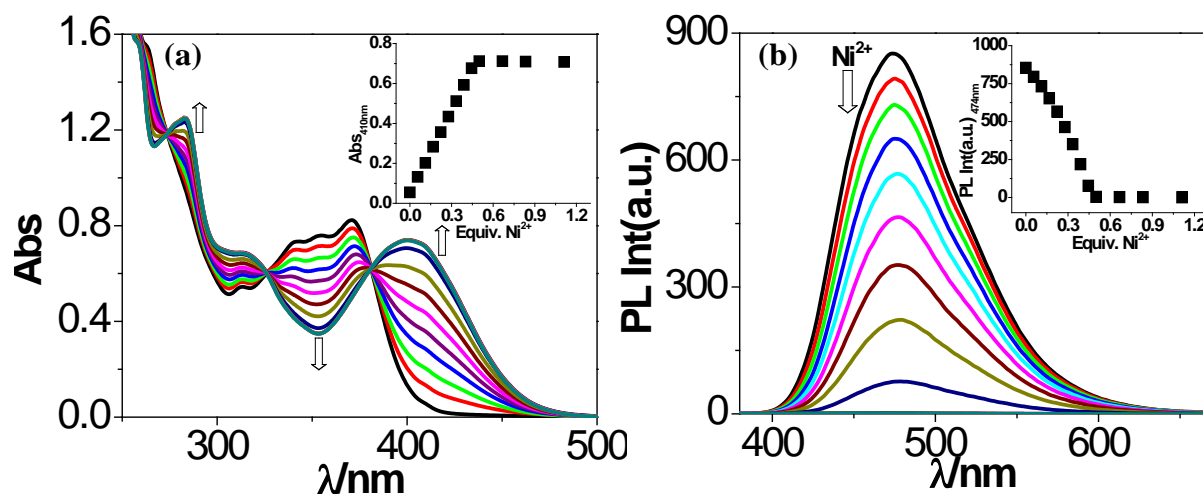


Fig. S18 Changes in UV-vis (a) and photoluminescence (b) spectra of tpy-HImzphen (20 μM) in dimethylformamide-acetonitrile (1:9) upon addition of $\text{Ni}(\text{ClO}_4)_2$ (20 μM). The inset shows the change of absorption and emission intensity as a function of the equivalent of Ni^{2+} ion added.

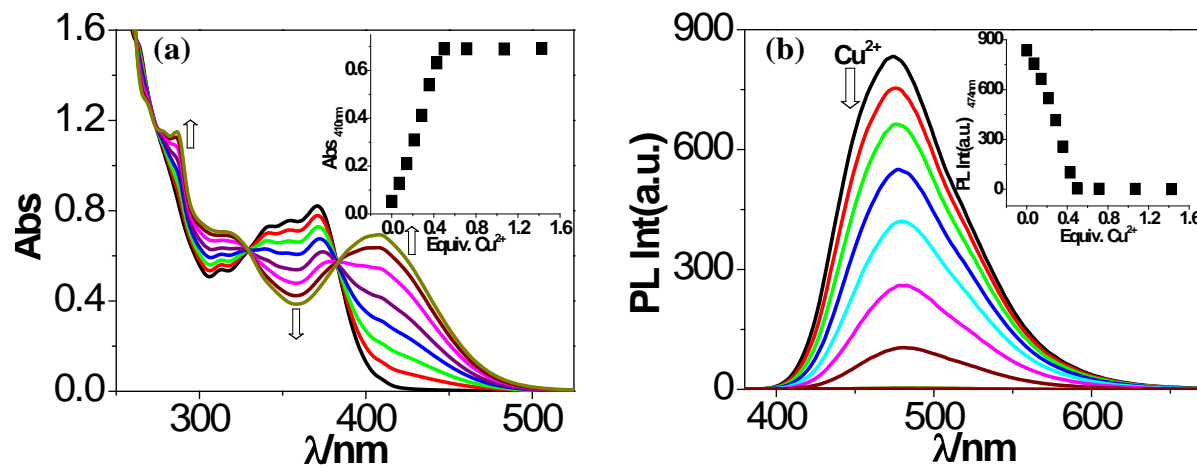


Fig. S19 Changes in UV-vis (a) and photoluminescence (b) spectra of tpy-HImzphen (20 μM) in dimethylformamide-acetonitrile (1:9) upon addition of $\text{Cu}(\text{ClO}_4)_2$ (20 μM). The inset shows the change of absorption and emission intensity as a function of the equivalent of Cu^{2+} ion added.

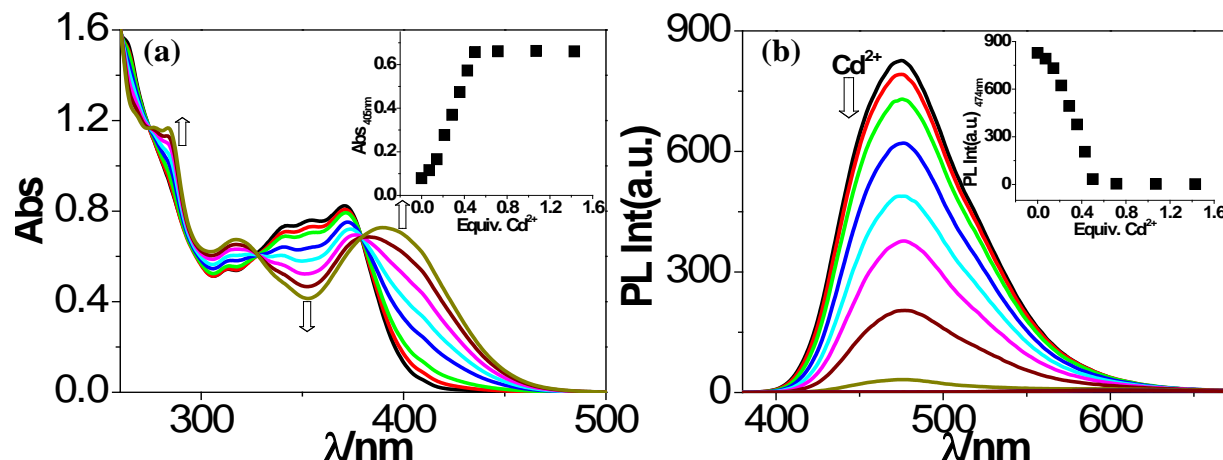


Fig. S20 Changes in UV-vis (a) and photoluminescence (b) spectra of tpy-HImzphen ($20 \mu\text{M}$) in dimethylformamide-acetonitrile (1:9) upon addition of $\text{Cd}(\text{ClO}_4)_2$ ($20 \mu\text{M}$). The inset shows the change of absorption and emission intensity as a function of the equivalent of Cd^{2+} ion added.

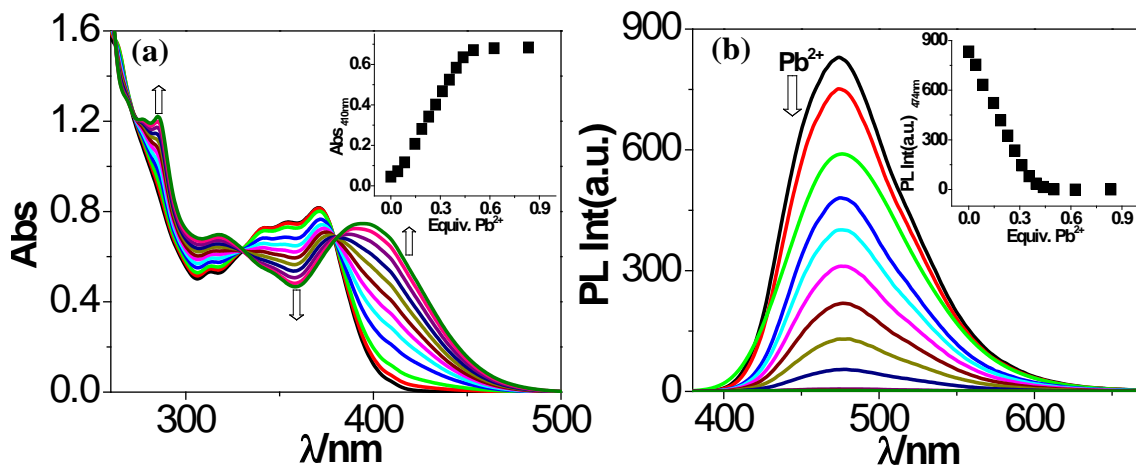


Fig. S21 Changes in UV-vis (a) and photoluminescence (b) spectra of tpy-HImzphen ($20 \mu\text{M}$) in dimethylformamide-acetonitrile (1:9) upon addition of $\text{Pb}(\text{ClO}_4)_2$ ($20 \mu\text{M}$). The inset shows the change of absorption and emission intensity as a function of the equivalent of Pb^{2+} ion added.

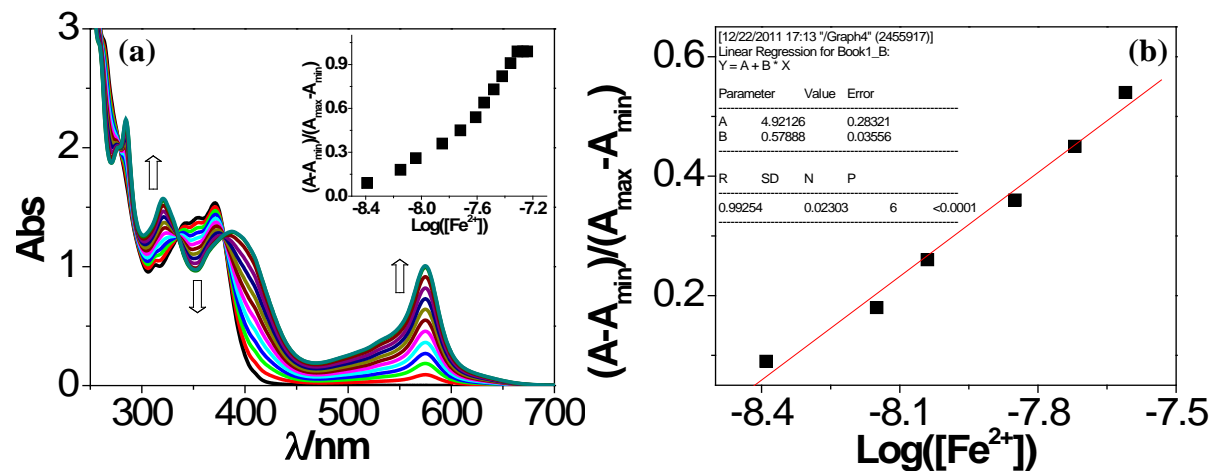


Fig. S22 (a) Absorbance changes during the titration of tpy-HImzphen (20 μM) with Fe^{2+} (0-20 μM) in dimethylformamide-acetonitrile (1:9), inset: Normalized absorbance between the minimum absorbance (free tpy-HImzphen) and the maximum absorbance (20 μM Fe^{2+} added). (b) A plot of $(A - A_{\min}) / (A_{\max} - A_{\min})$ vs $\text{Log}([\text{Fe}^{2+}])$, the calculated detection limit of receptor is $3.9 \times 10^{-9} \text{ M}$.

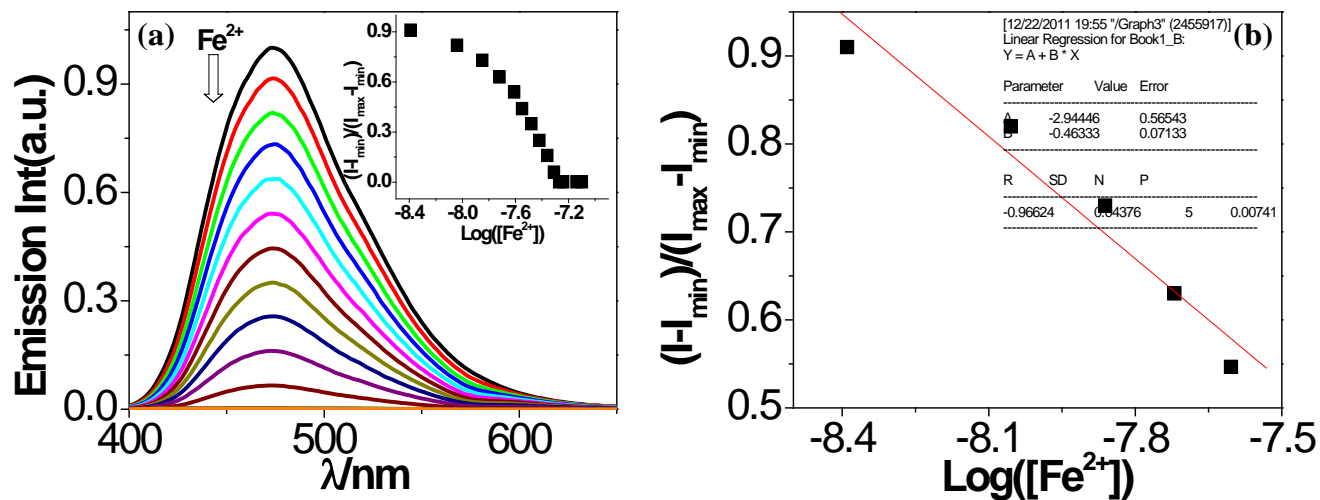


Fig. S23 (a) Fluorescence changes during the titration of tpy-HImzphen (20 μM) with Fe^{2+} (0-20 μM) in dimethylformamide-acetonitrile (1:9), inset: Normalized intensity between the maximum intensity (free tpy-HImzphen) and the minimum intensity (20 μM Fe^{2+} added). (b) A plot of $(I - I_{\min}) / (I_{\max} - I_{\min})$ vs $\text{Log}([\text{Fe}^{2+}])$, the calculated detection limit of receptor is $3.89 \times 10^{-9} \text{ M}$.

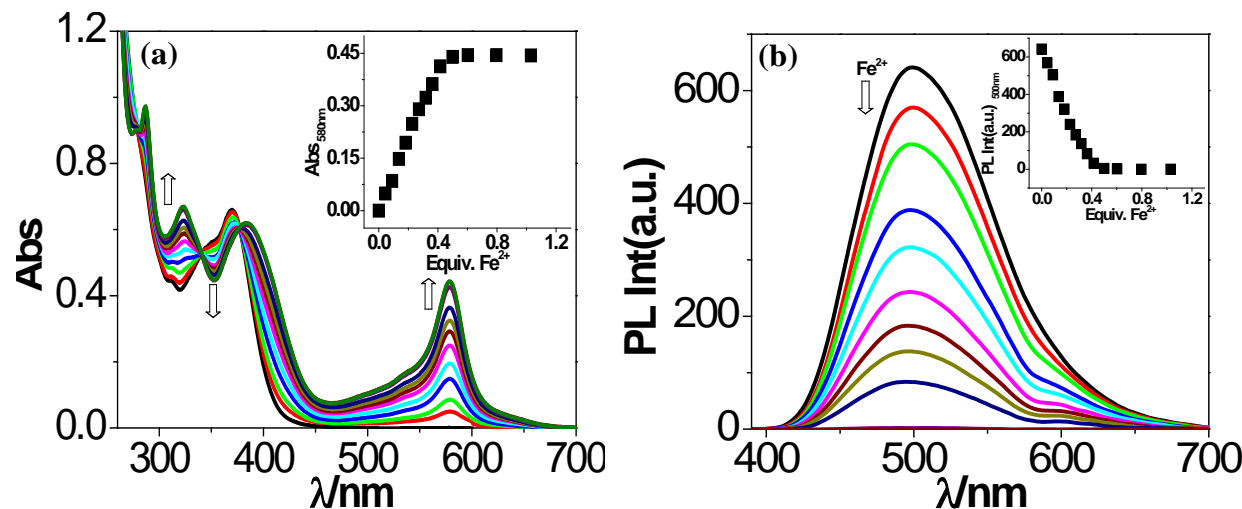


Fig. S24 Changes in UV-vis (a) and photoluminescence (b) spectra of tpy-HImzphen (20 μM) in dimethylsulfoxide-water (3:2) upon addition of $\text{Fe}(\text{ClO}_4)_2$ (22 μM). The inset shows the change of absorption and emission intensity as a function of the equivalent of Fe^{2+} ion added.

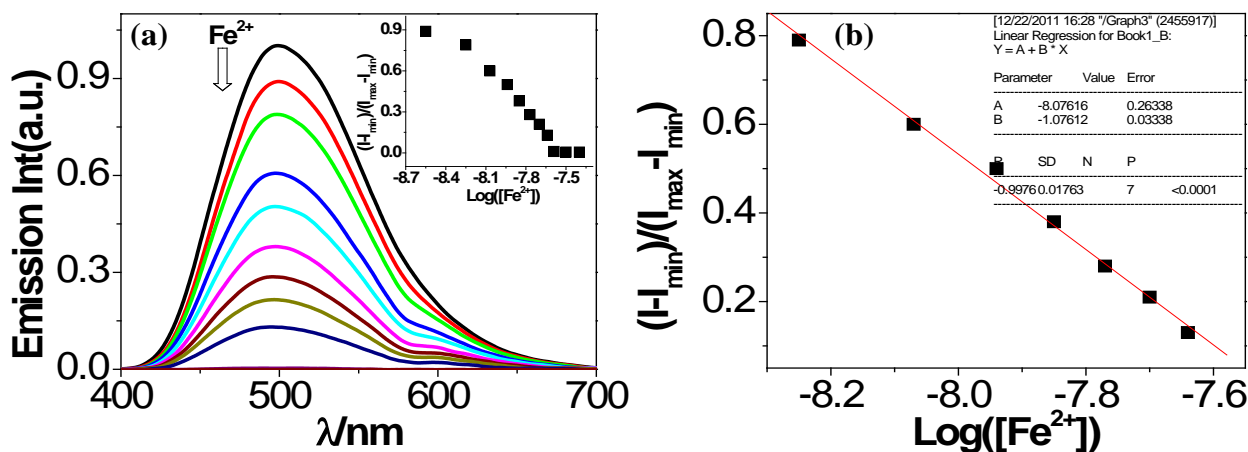


Fig. S25 (a) Fluorescence changes during the titration of tpy-HImzphen (20 μM) with Fe^{2+} (0-22 μM) in dimethylsulfoxide-water (3:2), inset: Normalized intensity between the maximum intensity (free tpy-HImzphen) and the minimum intensity (22 μM Fe^{2+} added). (b) A plot of $(I - I_{\min}) / (I_{\max} - I_{\min})$ vs $\log([\text{Fe}^{2+}])$, the calculated detection limit of receptor is $5.0 \times 10^{-9} \text{ M}$.